

To be submitted to
Zeitschrift für Physik A

ISTITUTO NAZIONALE DI FISICA NUCLEARE
Laboratori Nazionali di Frascati

LNF-81/5(P)
28 Gennaio 1981

A. El-Naghy · FRAGMENTATION OF ^{12}C NUCLEI
IN EMULSION AT 50 GeV/c.

A. El-Naghy (*): FRAGMENTATION OF ^{12}C NUCLEI IN EMULSION AT 50 GeV/c.

SUMMARY

A total of 852 ^{12}C -emulsion interactions at 4.2 GeV/nucleon have been investigated. In 86% of these events, at least one projectile fragment, was observed in each. The angular distributions of $Z=1,2$ and ≥ 3 projectile fragments are narrow and the dispersion of the distribution decreases with the increasing of Z . The production cross section of the reaction $^{12}\text{C} + \text{Em} \rightarrow 2 \text{Li}$ (from the projectile) + anything is about $6 \times 10^{-3} \sigma_{\text{in}}$. The only-projectile-fragmentation, $n_{\text{h}}=0$, events were studied in details. The percentage of these events is 10% of the total inelastic events. The events, in which α -fragment is the maximum charged emitted projectile fragment, have the maximum probability. This indicates that the projectile nuclear structure plays an important role in the fragmentation process. In 1.2% of the total events, ^{12}C has been dissociated into 3 α -particles.

The average number of produced charged pions per interacting projectile nucleon is constant at different impact parameters and equals the corresponding value from elementary interaction. This gives an evidence that nucleus-nucleus interaction can be considered as a superposition of nucleon-nucleon collision. The longitudinal momentum distributions of $Z=1$ and $Z=2$ projectile fragments are Gaussian shaped, narrow, consistent with isotropy in the projectile rest frame and depend on the fragment. These distributions are consistent with quantum mechanical calculations using the sudden approximation and shell-model functions.

A total of 852 ^{12}C -emulsion nucleus interactions at 4.2 GeV/c per incident nucleon have been investigated. The events in which at least one charged projectile fragment is observed are 733 event. In these events, the multiplicity and angular distributions of $Z=1,2$ and ≥ 3 projectile fragments were studied. Five events, in which ^{12}C projectile nuclei have been fragmented into two $Z=3$ fragments, were observed. Thus the cross section of this process is about 6×10^{-3} of the inelastic cross section. The angular distribution of projectile fragments becomes narrower as the fragment charge increases. At all values of fragment charges, a pronounced peak in the angular distribution is observed at zero emission angle. The only-projectile-fragmentation events which possess no heavily ionizing particle, i.e. $n_{\text{h}}=0$ events, are the main subject of this paper. The number of such events in our sample is 84 events i.e. about 10% of the total inelastic events. The numbers of events with Z_{max} , the charge of the emitted principal fragment, equals to 1,2,3,4 and 5 are 11,52,13,4 and 4 respectively. Out of these 84 events, 36 interactions have a total charge of the emitted projectile fragments Z^* equal to 6 i.e. as

(* Permanent address: Physics Department, Faculty of Science, Cairo University, Cairo, Giza, Egypt.

much as the beam charge Z_p . From these 36 events, 17 have no charged pions produced and out of these 17 events, 10 only represent the dissociation of $^{12}\text{C} \rightarrow 3\alpha$ i.e. 1.2% of the total inelastic interactions. The numbers of events with $Z^*=5,4,3,2$ and 1 are 27,14,4,2 and 1 respectively. The average number of produced charged pions per one interacting projectile nucleon was estimated to be 1.2 ± 0.1 . This value agrees with the corresponding one in elementary interaction at the same energy per nucleon, a result which pertains to the incoherent production model in collision of two nuclei. In this class of events, $n_h=0$, the number of stars in which H, He, Li, Be and B isotopes were detected are 59, 58, 13, 4 and 4 respectively. The projected angular distributions of $Z=1$ and 2 projectile fragments are Gaussian shaped, narrow, consistent with isotropy and depend on the fragment. These distributions are consistent with a quantum mechanical calculations using the sudden approximation and shell-model functions. From the angular measurements of α -particle tracks in the dissociation $^{12}\text{C} \rightarrow 3\alpha$ events, the distribution of α -particle transverse momentum inside the carbon projectile nucleus was deduced. It seems that the dissociation of $^{12}\text{C} \rightarrow 3\alpha$ happens via an intermediate ^8Be state.

1. INTRODUCTION

Experimental study of nucleus-nucleus interactions became possible after the discovery of heavy nuclei in primary cosmic rays about thirty years ago /1/. In spite of the uncertainty in charge and energy determination of the heavy primaries, cosmic ray experiments have revealed the general characteristics of nucleus-nucleus interactions /1-8/.

The recent availability of relativistic nuclear beams from the accelerators at the Lawrence Berkeley Laboratory and Joint Institute for Nuclear Research makes it possible to investigate and deepen our understanding of nucleus-nucleus interactions at high energies. Such studies are very important for simulations of cosmic ray showers produced by heavy primaries. Accurate knowledge of the interaction mean free path and fragmentation probabilities is needed for these simulations /9-11/.

The nucleus-nucleus interactions are also interesting because they provide much more information about the elementary nucleon-nucleon process than in the case of hadron-nucleus collisions. In the collision of two nuclei, the elementary interaction is more amplified than in the case of hadron-nucleus interaction. It is worthy to refer, here, to our previous papers /12,13/ in which this idea and others about collective interactions and shock waves were discussed using the most central collisions between nuclei. These works had shown that nucleus-nucleus interaction can be considered as a superposition of nucleon-nucleon collisions.

At such high energy (4.2 GeV/nucleon) the rapidity gap between the projectile and target fragmentation regions is quite wide. This provides us with a good possibility for testing the limiting fragmentation hypothesis which implies that no correlations exist between the projectile and target fragments. In /14-16/, fragmentation of relativistic heavy ions at 1.05 and 2.1 GeV/ nucleon was studied and it was shown that the modes of projectile fragmentation are target independent. These results were obtained from the study of single-particle inclusive experiments where the degree of target fragmentation can take any value. It is interesting to compare these results with those of projectile fragments angular distributions from the special class of events, $n_h=0$, where there is no target fragmentation but only a projectile fragmentation. In /17/ such analysis was made for collisions of ^4He , ^{12}C , ^{14}N , and ^{16}O nuclei with emulsion at 2.1 GeV/nucleon. The comparison of our data with the previous ones, gives a possibility to test the energy and projectile mass dependences. Thus this paper is devoted to the study of projectile fragments with a special attention to the class of events, $n_h=0$, in which the target nucleus is unwounded (not fragmented).

2. EXPERIMENT

Stacks of 600 μm thick Br-2 nuclear emulsions were exposed to the 4.2 GeV/c per incident nucleon ^{12}C beam at the Dubna Synchrophasotron. Only very thick dark beam tracks, apart from the surface and bottom by at least 50 μm (undeveloped emulsion), were chosen for along the track double scanning, fast in the forward and slow in the backward direction. Thus, we raised the scanning efficiency nearly to 100% and picked up mostly all events having the difference between the charges of the projectile and the principal projectile fragment $\Delta Z = Z_P - Z_F < 2$ which could escape detection in case of forward scanning only. Also, we minimized as much as possible the scanning of beam tracks of $Z_P \leq 5$ light nuclei. However, the scanned beam tracks were further examined by measuring the δ -electron density on each of them. The negligible fraction of beam particles having $Z \leq 5$ were thus identified and excluded from our data. The one-prong events, with an emission angle of secondary particle track $\theta \leq 3^\circ$ and without visible tracks from excitation or disintegration of the incident particle and/or target nucleus, were excluded as due to elastic scattering.

Along the total scanned length of 337.9 m, 2468 inelastic interactions of ^{12}C ions with emulsion were recorded, leading to the mean free path for inelastic interaction $\lambda = 13.7 \pm 0.3$ cm. This value and other experimental data were compared with theoretical predictions in our previous paper /12,13,18/. The comparison had shown that the calculations carried out according to geometric models /19,20/ are in a satisfactory agreement with the experimental cross sections.

For the present analysis 852 inelastic interactions of ^{12}C ions with emulsion at 4.2 GeV/nucleon were used. The charged secondary particles, in these events, were classified into the following:

- 1) Relativistic particles or showers (s) of relative ionization $g/g_0 < 1.4$, where g is the particle track ionization and g_0 is the ionization at the "plateau". Tracks of such type but with an emission angle $\theta \leq 3^\circ$ were further subjected to rigorous multiple scattering measurement for momentum determination and consequently for separating produced pions from single charged projectile fragments (protons, deuterons and tritons) /12,13,18/. About 10% of the measured tracks were identified as pions, 70% protons 15% deuterons and 5% tritons.
- 2) Grey particle tracks (g) with $L > 3$ mm and $g/g_0 > 1.4$ and having dip angle $\alpha \leq 30^\circ$.
- 3) Black particle tracks (b) with $L \leq 3$ mm and $\alpha \leq 30^\circ$. In order to take into account g and b tracks with $\alpha > 30^\circ$ a geometrical weighting factor W was attached to every b and g particle track, such that

$$W = 1 \quad \text{when } 150^\circ \leq \theta \leq 30^\circ$$

otherwise

$$W = \pi/2 \text{ arc sin } (\sin 30^\circ / \sin \theta)$$

To distinguish between g and b particles and projectile multiply charged fragments, we define two further types of particles.

- 4) Double-charged $Z=2$ projectile fragments with $g/g_0 \simeq 4$, $\theta \leq 3^\circ$ and without any change in ionization along a length of at least 2 cm from the interaction vertex. For more confirmation of this criterion the ionization of these tracks were compared to the distinguishable tracks of events $^{12}\text{C} + A \rightarrow A + 3\alpha$ where A is an emulsion nucleus.
- 5) Multicharged $Z \gg 3$ projectile fragments having relative ionization $g/g_0 = 6$, $\theta \leq 3^\circ$ and without any change in ionization along a length of at least 1 cm from the vertex. Further, the δ -electron density was measured for these tracks and they were subdivided into $Z=3, 4$ and 5 fragments.

Thus we adequately divided the emitted particles into projectile and target fragments. Moreover the projectile fragments are divided into $Z=1, 2, 3, 4$ and 5 charged fragments. The $Z=1$ fragments are subdivided into protons, deuterons and tritons. Target fragments are divided into fast shower particles s and slow heavily ionizing

h particles.

In each star the total charge of the projectile fragments, $Z^* = \sum_i N_i Z_i$, was estimated where N_i is the number of fragments having charge Z_i in the given event. Also, the number of projectile interacting nucleons in each event, $\nu = 12 - 2Z^*$, was determined.

It is to be noted that, in contrast to /17/, we have the advantage of dividing $Z=1$ shower particles into pions, protons, deuterons and tritons. Moreover, the multi-charged fragments are divided into $Z=2,3,4$ and 5 fragments.

3. FRAGMENTATION PARAMETERS

3.1. Multiplicities of Fragments

In the present paper 852 ^{12}C inelastic interactions with emulsion were measured, 733 events were observed to have emitted projectile fragments i.e. 86% of the total events represent peripheral and quasiperipheral collisions. This percentage is about two times larger than the corresponding one in interactions of α -particle with emulsion /21/ at the same energy per nucleon. The multiplicity distributions of the emitted charged projectile fragments are shown in Fig. 1 (a,b,c) with the corresponding distributions from ^{14}N interactions with emulsion at 2.1 GeV/nucleon /27/. It is seen that for $Z=1$ fragments, there is a good agreement between the two

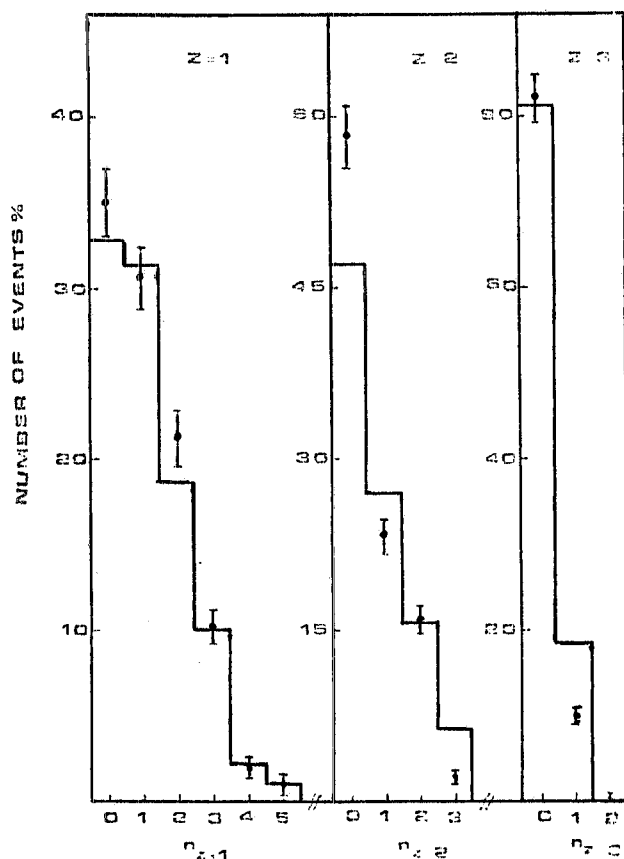


FIG. 1 - The multiplicity distributions of charged projectile fragments : a) $Z=1$, b) $Z=2$, c) $Z=3$. The histogram represents data of ^{14}N -emulsion interactions /2/ and the dots are our experimental points. Fragments of $Z \geq 4$ constitute $(6.5 \pm 1.5)\%$ of the total events.

distributions. For $Z=2$ fragments, except the first interval of zero multiplicity in which there is a difference of about one statistical error, the agreement is satisfactory. In Fig. 1(c), it seems that there is a difference in the second interval of the distribution but if we realize that in /22/, the charged projectile fragments of $Z > 3$ were not analyzed and they are included in this distribution, the agreement will be striking. The percentage of events with one fragment of charge $Z \geq 3$, in our sample, is $(17.3 \pm 1.4)\%$ which agrees with the corresponding value from ^{14}N interactions in emulsion. The distributions of Fig. 1 show that, within this short range of energy, the

projectile fragmentation is energy independent. In /17/, studying the fragmentation of ^{12}C , ^{14}N and ^{16}O nuclei in emulsion, the authors did not observe single event in which two projectile fragments of $Z \geq 3$ are emitted and they deduced that the cross section of such process is less than 10^{-3} of the inelastic cross section. In this experiment we observed five events in which ^{12}C has been fragmented into two $Z=3$ fragments. In these five events, charged pions have been produced and only one of them has $n_h=0$. This means that in these reactions, may be a projectile neutron has interacted. The cross section of this reaction is about 6×10^{-3} of the inelastic cross section. This value contradicts the result of /17/, in which fragment charges were measured by the blob density method. It is to be noted, here, that in our experiment the separation of $Z=2$ and $Z=3$ fragments was rigorously tested by the claibrating tracks of carbon dissociation into 3α particles. The only possible error in $Z=3$, if any, will be in the side of its increasing i.e. $Z=4$ which does not change the final result.

3.2. Angular Distributions

Fig. 2 represents the angular distributions of $Z=1,2$ and ≥ 3 particle fragments, in terms of $\cos \theta$, where θ is the space angle between the emitted projectile fragment and the beam direction. It can be seen clearly that the angular distribution becomes narrower with the increasing of fragment charge Z . The dispersions of these distributions are 1.4×10^{-7} , 4.0×10^{-8} and 8.6×10^{-9} for $Z=1,2$ and ≥ 3 respectively. In all these distributions there are pronounced peaks at $\cos \theta=1$. These behaviours were observed before in the early cosmic ray experiments /3,4/.

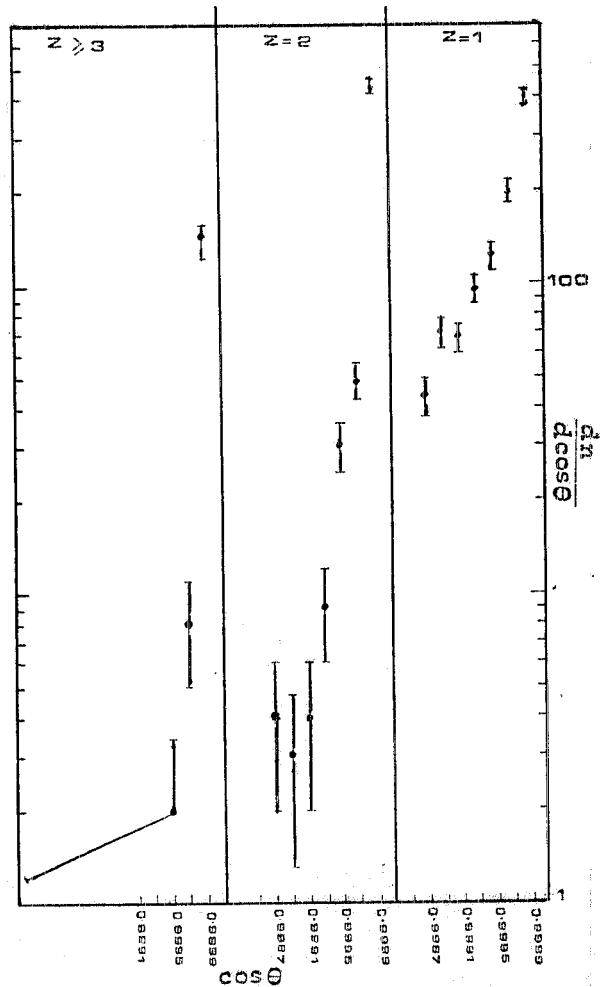


FIG. 2 - The angular distributions of $Z=1,2$ and ≥ 3 projectile fragments.

4. EVENTS WITH PROJECTILE FRAGMENTATION ONLY

The motivation for the choice of $n_h=0$ events for detailed study is the comparison of their high-rapidity projectile fragment angular distributions with the results of the single particle inclusive experiments /14-16/, where there were no restrictions on the fragmentation of the target. This comparison provides a more stringent test of the limiting fragmentation hypothesis. The only work of this kind was carried out by Heckman et al. /17/ at 2.1 GeV/nucleon. It is interesting to compare our data at 4.2 GeV/nucleon with this work.

In the 84 events, satisfying the criterion $n_h=0$ from our sample of 852 inelastic interactions, the projectile fragments are divided into $Z=1,2,3,4$ and 5. The $Z=1$ fragments are subdivided into protons, deuterons and tritons.

No experimental trial was made to separate isotopes of $Z=1$ fragments. In Table I, we list explicitly all the observed reaction products of these 84 events. They are ordered according to the value of Z^* , the total charge of the emitted projectile fragments. It is to be kept in mind that neutrons and neutral pions may be emitted in all these reactions.

TABLE I - Catalog of the observed charged particles produced in the 84 events of $n_h=0$, ordered according to the value of Z^* .

Z^*	Reaction products	frequency	Z^*	Reaction products	frequency	Z^*	Reaction products	frequency
1	$^1\text{H} + 6\pi$	1	5	$5^1\text{H} + 2\pi$	1	6	$2\text{He} + ^2\text{H} + ^1\text{H}$	1
	$2^1\text{H} + 9\pi$	1		$2^2\text{H} + 4^1\text{H} + 2\pi$	1		$\text{He} + ^3\text{H} + ^2\text{H} + 2^1\text{H}$	1
2	$\text{He} + 2\pi$	1	5	$\text{He} + ^3\text{H} + 2^1\text{H} + 4\pi$	1	6	3He	10
				$\text{He} + 3^1\text{H} + 4\pi$	1		$\text{Li} + \text{He} + ^2\text{H}$	1
3	$3^1\text{H} + 4\pi$	1	5	$2\text{He} + ^3\text{H} + \pi$	3	6	Be+He	1
	$2^2\text{H} + ^1\text{H} + 4\pi$	1		$2\text{He} + ^2\text{H} + 4\pi$	1		$\text{B} + ^3\text{H}$	1
	$2^2\text{H} + 2^1\text{H} + 5\pi$	2		$2\text{He} + ^2\text{H} + \pi$	2		$\text{B} + ^2\text{H}$	1
4	$2^2\text{H} + 3^1\text{H} + 5\pi$	1	5	$2\text{He} + ^1\text{H} + 4\pi$	2	6	$\text{He} + ^3\text{H} + ^2\text{H} + 2^1\text{H} + \pi$	1
	$2^2\text{H} + 3^1\text{H} + 3\pi$	1		$2\text{He} + ^1\text{H} + 3\pi$	1		$2\text{He} + ^2\text{H} + ^1\text{H} + \pi$	1
	$4^1\text{H} + 4\pi$	1		$2\text{He} + ^1\text{H} + 2\pi$	5		$2\text{He} + 2^1\text{H} + 2\pi$	4
	$\text{He} + ^2\text{H} + ^1\text{H} + 3\pi$	2		$2\text{He} + ^1\text{H} + 6\pi$	1		$2\text{He} + 2^1\text{H} + \pi$	4
	$\text{He} + ^2\text{H} + ^1\text{H} + 4\pi$	1					$2\text{He} + 2^1\text{H} + 3\pi$	2
	$\text{He} + 2^1\text{H} + 3\pi$	1		$\text{Li} + \text{He} + \pi$	3		$2\text{He} + 2^1\text{H} + 4\pi$	1
	$\text{He} + 2^1\text{H} + 4\pi$	2		$\text{Li} + ^2\text{H} + ^1\text{H} + 2\pi$	1		3He+3 π	1
	$2\text{He} + \pi$	1		$\text{Li} + 2^1\text{H} + 3\pi$	2			
	$2\text{He} + 3\pi$	1					$\text{Li} + 2^1\text{H} + ^2\text{H} + \pi$	1
	$\text{Li} + ^2\text{H} + 2\pi$	1		$\text{Be} + ^1\text{H} + 3\pi$	1		$\text{Li} + \text{He} + ^1\text{H} + \pi$	2
$\text{Li} + ^2\text{H} + 3\pi$	1			2Li+3 π	1			
$\text{Be} + 4\pi$	1	$\text{B} + 2\pi$	1					
						$\text{Be} + \text{He} + 3\pi$	1	

4.1. Topological Features of the Fragmentation Process.

From Table I, we can extract various features of the fragmentation process. The production frequency of events in ^{12}C -emulsion interactions as a function of Z_{max} , the highest charged projectile fragment emitted in the interaction, is shown in Fig. 3. It is to be noted that the maximum probability is for events with $Z_{\text{max}}=2$ i.e. with α -particle projectile fragment as the maximum emitted charged projectile fragment. This is interpreted as due to the structure of ^{12}C nucleus which is an even-even nucleus of total spin $I=0$. This means that the nuclear structure of the projectile may play an important role in the fragmentation process. The authors of [15,16] observed effects, attributable to the structure of fragment nuclei, in the systematics of the longitudinal momentum distributions and isotope production cross section. Table II gives the percentage frequency of

TABLE II - Production frequency, in percent, of events in emulsion as a function of Z_{\max} , the highest charged projectile fragment produced in an interaction.

Z_{\max} energy/nucleon	1	2	3	≥ 4
2.1 GeV/nucleon	7 ± 2	59 ± 10	8 ± 3	26 ± 12
4.2 GeV/nucleon	13 ± 4	62 ± 9	15 ± 4	10 ± 3

production of $Z_{\max}=1,2,3$ and ≥ 4 in this class of events, $n_h=0$, from interactions of ^{12}C with emulsion at 2.1 GeV/nucleon /17/ and 4.2 GeV/nucleon. These values, within the large statistical errors, are in an agreement which indicates the energy independence of the distribution in this range of energy.

Fig. 4 represents the frequency distribution of Z^* , the total charge of the emitted projectile fragments in an interaction, for our sample of $n_h=0$ events. The distribution is smooth and the frequency decreases with the value of Z^* . The average value of Z^* equal 5.05 ± 0.12 and the average number of produced charged pions, in these events, equals 2.20 ± 0.10 . From Fig. 4, the average number of interacting projectile nucleons $\langle \nu \rangle = 1.90 \pm 0.24$, thus the average number of produced charged pions per one interacting nucleon $\langle n_{\pi} \rangle / \langle \nu \rangle = 1.16 \pm 0.20$. This result gives an evidence for the incoherent production model /23/ in collision of two nuclei. The constancy of the average number of produced pions per one interacting projectile nucleon was also indicated in our previous works /12,13,18/.

Fig. 5 represents the n_{π} and Z^* distributions for events with $Z_{\max}=1,2$ and ≥ 3 . The n_{π} -distributions, for all values of Z_{\max} , are flat and show no pronounced peak or special structure. The Z^* -distributions, for $Z_{\max}=2$ and ≥ 3 , have an increasing at $Z^*=6$. This means that most of the interactions, in these events, are due to projectile neutrons. The $Z_{\max}=1$ sub-class of events has no single event with $Z^*=6$ which shows that the complete break-up of projectile nucleus into individual nucleons is very seldom. From Fig. 5, we deduce the average values of: produced charged pions $\langle n_{\pi} \rangle$, total charge of the emitted projectile fragment $\langle Z^* \rangle$, interacting projectile nucleons $\langle \nu \rangle$ and number of charged produced pions per one interacting projectile nucleon $\langle n_{\pi} \rangle / \langle \nu \rangle$. These data, ordered according to Z_{\max} , are given in Table III. The attention is attracted to the observed constancy,

TABLE III - The average values of: number of produced charged pions, total charge of emitted projectile fragments, number of interacting projectile nucleons and the number of produced charged pions per one interacting nucleon.

Z_{\max} Average values	1	2	≥ 3
$\langle n \rangle$	4.5 ± 0.6	1.9 ± 0.2	1.6 ± 0.3
$\langle Z^* \rangle$	3.4 ± 0.4	5.3 ± 0.1	5.3 ± 0.2
	5.3 ± 0.7	1.4 ± 0.2	1.3 ± 0.3
$\langle n_{\pi} \rangle / \langle \nu \rangle$	0.9 ± 0.2	1.3 ± 0.4	1.2 ± 0.5

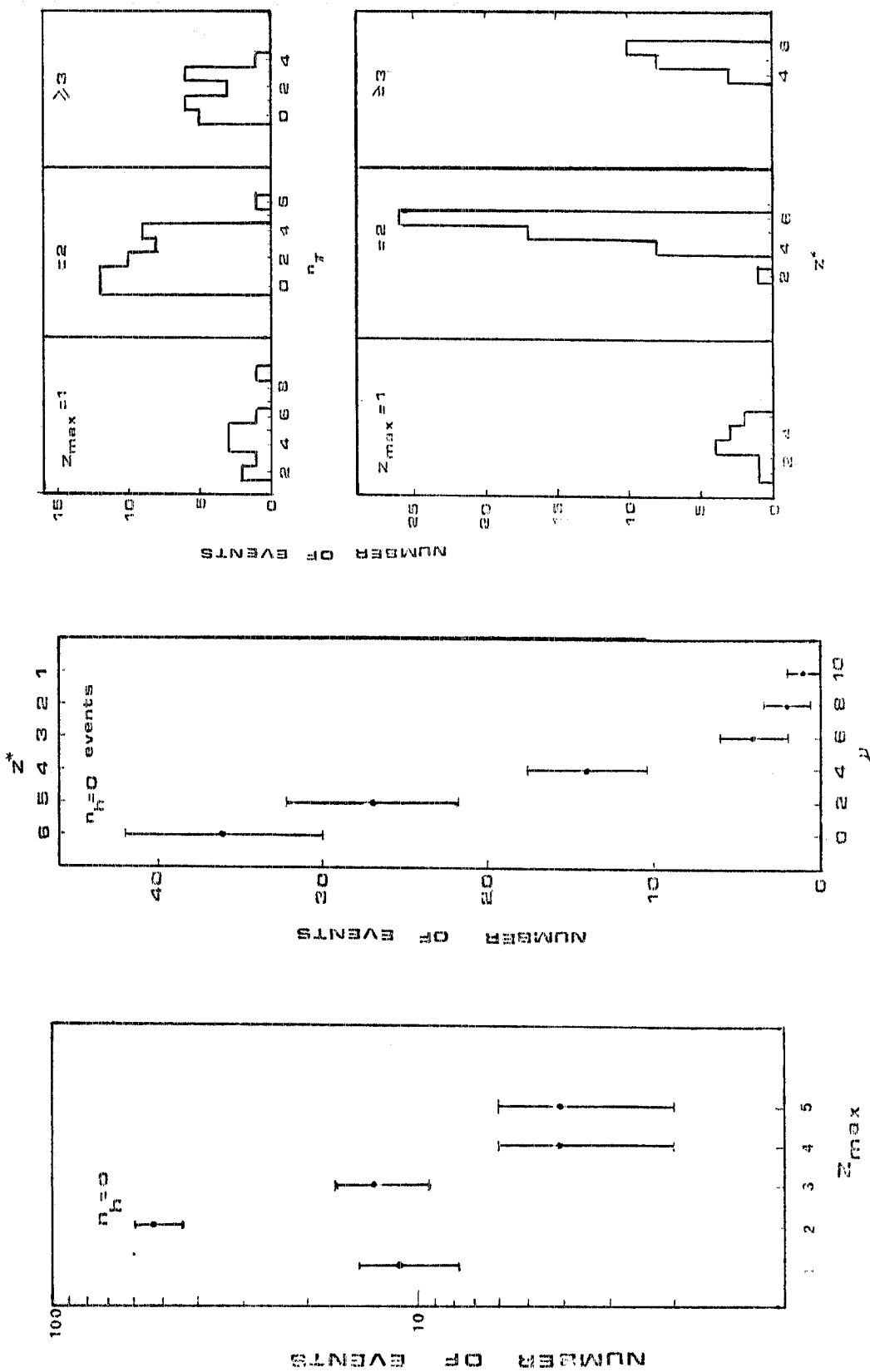


FIG. 3 - The production frequency of $n_h=0$ events as a function of Z_{max} , the highest charge of a projectile fragment in an event.

FIG. 4 - The production frequency of $n_h=0$ events as a function of Z , the total charge of the emitted projectile fragments in event.

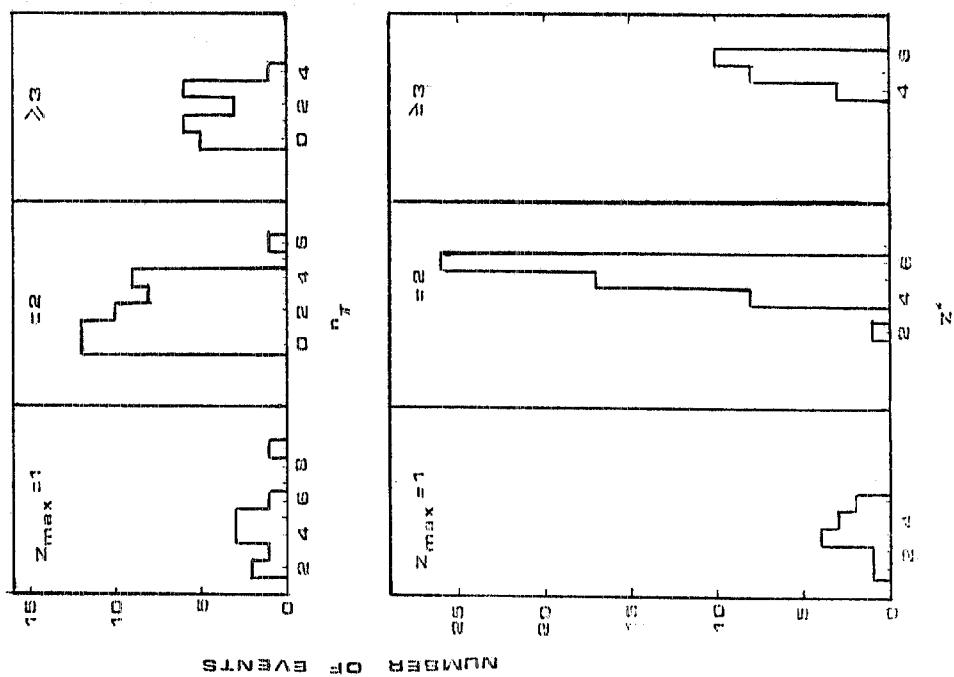


FIG. 5 - The n_h , n_{12} and Z^* distributions for the fragmentation of ^{12}C nuclei in nuclear emulsion, $n_h=0$ events. The data are ordered according to Z_{max}^1 .

within errors, of the average number of produced charged pions per interacting projectile nucleon in all these sub-classes. This result gives more confirmation for our previous conclusion about considering nucleus-nucleus interaction a superposition of nucleon-nucleon collisions.

4.2. Angular Distributions of Particles Emitted in the Fragmentation Process.

In high energy nucleus-nucleus interactions, some of the projectile nucleons pass without interaction and they usually have the same projectile rapidity, these nucleons are called projectile "spectators". Target nucleons, not sharing in the interaction process are called target "spectators". Nucleons from both projectile and target, participating in the interaction, are called projectile and target "actors". When a nucleon is no longer a spectator but an actor, it takes any dynamically allowed value of rapidity between projectile and target fragmentation regions. In this class of events, $n_h=0$, we expect that the rapidity distribution is dominated by the projectile fragments which carry the same rapidity as the projectile. Fig. 6 illustrates the rapidity ($\eta = -\ln \tan \theta/2$) distribution for all shower tracks (pions and hydrogen isotopes) emerged from stars of $n_h=0$, in comparison with the corresponding distribution of shower tracks from central events i.e. events with $Z^*=0$. A pronounced rapidity gap is observed between the two distributions. The distribution of central events extends from the target fragmentation region to the projectile fragmentation region. This is due to the absence of spectator and the complete dominance of actors. The distribution from $n_h=0$ events is dominated by the projectile spectators, thus it is mainly concentrated in the projectile fragmentation region. These features pertain to the limiting fragmentation hypothesis.

The authors of /24/ have treated the fragmentation of high-energy nuclei by a quantum mechanical calculation using the sudden approximation and shell model functions. They have shown that projected momentum distributions in the projectile frame are to a good approximation, Gaussian with standard deviation widths, to a first order, given by

$$\Delta = \left[m \omega A_F (A_p - A_F) / 2 A_p \right]^{1/2} \text{ MeV} \quad (1)$$

where

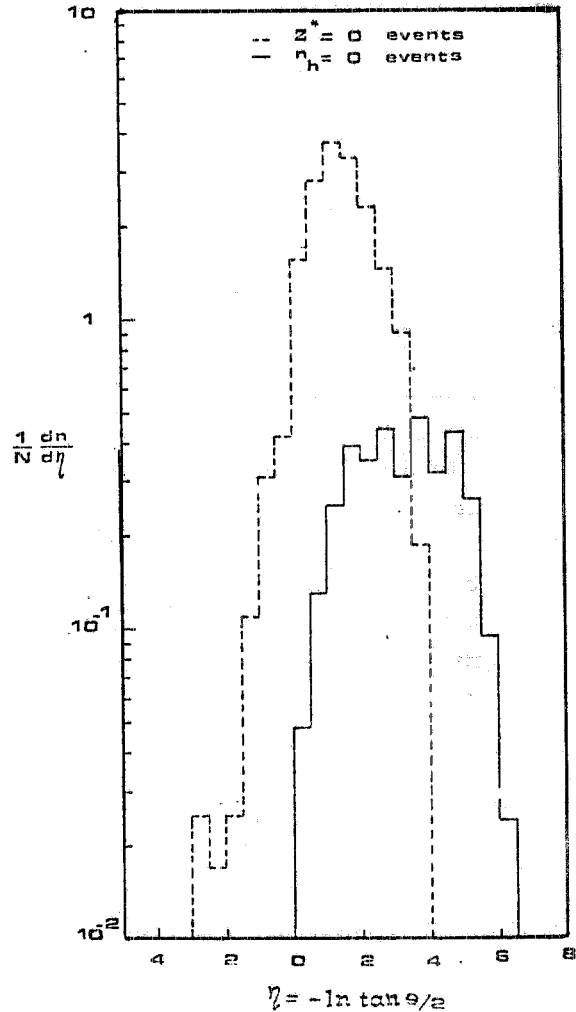


FIG. 6 - The rapidity ($\eta = -\ln \tan \theta/2$) distributions of shower tracks from central events, $Z^*=0$, and from the projectile fragmentation, $n_h=0$, events:

A_p is the mass number of the projectile nucleus,
 A_F is the fragment mass number,
 m is the proton mass in MeV,
 and $\omega = 45 A_p^{-1/3} - 25 A_p^{-2/3}$.

It is interesting to compare our experimental data with these theoretical predictions.

Fig. 7 represents the projected angular distribution of all shower tracks emitted from $n_h=0$ events in our sample, in comparison with the corresponding distribution from ^{12}C , ^{14}N and ^{16}O collisions with emulsion at 2.1 GeV/nucleon. The projection angle θ is defined as the angle between the projection of the emitted particle track in the emulsion plane (the x-y plane) and the beam direction (the beam is along the microscope x-axis). There is a pronounced peak at the first interval i.e. at the first five degrees. This peak obviously due to the projectile singly-charged fragments (hydrogen isotopes). Unlike the work /17/, the shower tracks, in our sample, are divided into pions and hydrogen isotopes. Fig. 8 represents the projected angular distribution of hydrogen isotopes in our sample of $n_h=0$ events. Fig. 9 shows the projected angular distribution of He isotopes. It is to be noted that the later distribution is restricted to the interval of 1.2° i.e. much narrower than the hydrogen isotopes distribution. To compare these two distributions with Eq. (1), the experimental points were fitted to a Gaussian distribution of the form $N(\theta) = \text{constant} \cdot \exp(-\theta^2/2\Delta^2)$. The results of fitting are shown in Figs. 8,9. The standard deviation widths Δ from the fitting are compared with theoretical predictions, calculated according to Eq. (1), in Table IV.

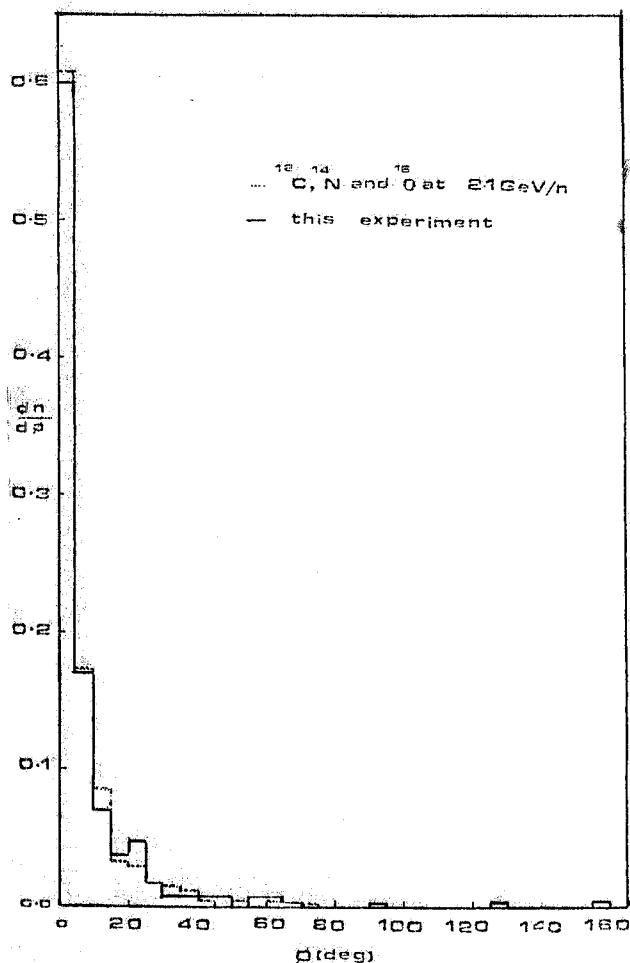


FIG. 7 - The projected angular distribution of shower tracks emitted from $n_h=0$ events. The dotted histogram represents data from ^{12}C , ^{14}N and ^{16}O interactions with emulsion at 2.1 GeV/nucleon. The continuous histogram represents our experimental data.

TABLE IV - Standard deviation widths of the momentum and projected angular distributions of Z=1 and Z=2 projectile fragments. The production-weighted angular widths are $\Delta_{Z=1}$ and $\Delta_{Z=2}$ respectively.

Isotope	Weight Wt	$\Delta_p(\text{MeV}/c)$	$\Delta_\theta(\text{deg.})$	This experiment
^1H	0.75	79	1.09	
^2H	0.18	107	0.74	
^3H	0.07	126	0.58	
		$\Delta_{Z=1}=87.4$	$\Delta_\theta=0.99$	$\Delta_\theta=0.92 \pm 0.08$
^3He	0.24	126	0.58	
^4He	0.76	138	0.47	
		$\Delta_{Z=2}=135.1$	$\Delta_\theta=0.50$	$\Delta_\theta=0.46 \pm 0.06$

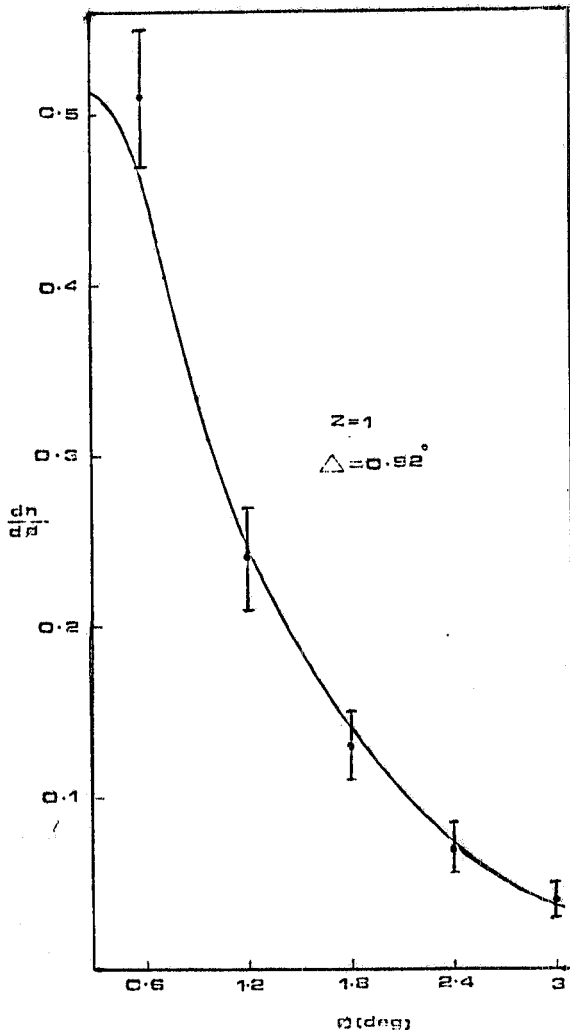


FIG. 8 - The projected angular distribution of hydrogen isotopes projectile fragments, the curve is a fitting of the experimental points to a Gaussian formula $N(\theta) = \text{const.} \exp -\theta^2/2\Delta^2$.

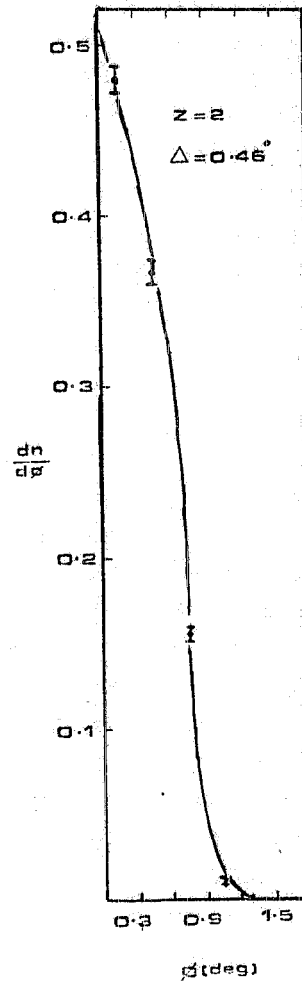


FIG. 9 - The projected angular distribution of He isotopes projectile fragments, the curve is a fitting of the experimental points to a Gaussian distribution.

In the calculation for $Z=1$ fragments we used a weight factor (Wt) for ^1H , ^2H and ^3H equal to their fractions as found in our sample of $n_p=0$ events. For $Z=2$ fragments the weights for ^3He and ^4He were taken from /17/. These results are summarized in Table IV which shows a good agreement of the experimental data with the predictions of /24/. This agreement was found also when analyzing the single-particle inclusive spectra /14-16/. In the later experiments the degree of target fragmentation could take any value, however it gave the same result as our data of unwounded (not fragmented) target. This is another strong evidence for the limiting fragmentation hypothesis which implies that both target and projectile are fragmented independent on each other. This result was also indicated in /17/.

6. THE DISSOCIATION OF $^{12}\text{C} \rightarrow 3\alpha$

This class of events is of particular interest. It consists of three-prong stars, each track of which is emitted within $\theta \leq 3^\circ$ of the beam direction and has a charge $Z=2$, determined by the δ -electron density method. From Table I, it is seen that we have only 10 events of this type in our sample of 852 inelastic interactions. Another 18 events were accumulated during the course of scanning, so our sample of these events includes 28 stars.

Assume that the momentum of each α -particle fragment emitted in a dissociated event is equal to one third of the projectile nucleus momentum P_0 . Consequently, the transverse momentum of each α -fragment

$$q_i = \frac{1}{3} P_0 \sin \theta_i \quad (2)$$

The vector sum of q_i , in each event, is equal to the transverse momentum transferred to the ^{12}C nucleus in the diffraction dissociation process. Consequently, to a first approximation, the transverse momentum of an α -particle inside the ^{12}C nucleus is given by

$$\vec{q}_i^* = \vec{q}_i - \frac{1}{3} \sum_{i=1}^3 \vec{q}_i \quad (3)$$

The distribution of α -particle transverse momentum inside the carbon projectile nucleus, q_i^* , is shown in Fig. 10, taken from our previous paper /18/.

Out of the 28 dissociation events, 18 have two α fragments emitted within a very narrow angle of the beam direction i.e. with a very low transverse momentum while the third α -fragment has a relatively larger angle, probably to compensate the sum of transverse momenta of the other two α -particles. This indicates that the dissociation of $^{12}\text{C} \rightarrow 3\alpha$ goes through an intermediate ^8Be state.

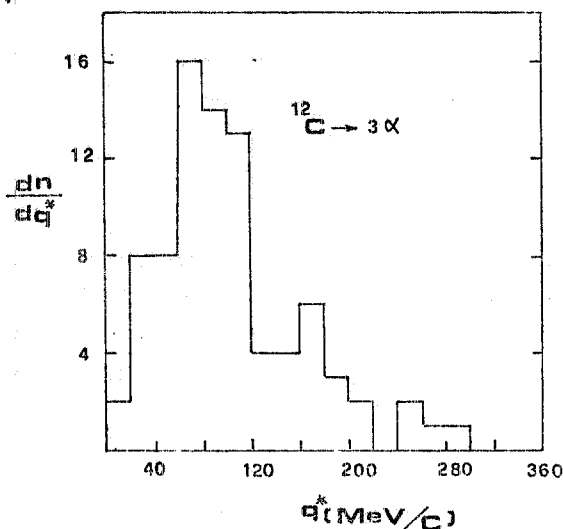


FIG. 10 - The transverse momentum distribution of α -particles inside the Carbon projectile nucleus as deduced from $^{12}\text{C} \rightarrow 3\alpha$ dissociation events.

7. CONCLUSIONS

From the study of the fragmentation of ^{12}C relativistic nuclei in emulsion at 4.2 GeV/nucleon, the followings can be concluded

- 1) In 86% of the total inelastic events, at least one projectile charged fragment is observed to be emitted in a star.
- 2) The cross section of the reaction $^{12}\text{C} + \text{emulsion} \rightarrow 2\text{Li}$ (projectile fragments) + anything is about 6×10^{-3} of the inelastic cross section.

- 3) The angular distributions of the projectile fragments are typically narrow and their dispersions decrease with the increasing of the fragment charge Z .

The only-projectile fragmentation events i.e. interactions having no emitted target fragments, $n_h=0$, are 10% of the total inelastic events. From the study of this special class of interactions, the following conclusions can be drawn:

- 1) The events in which α -fragment is the maximum charged emitted projectile fragment, have the maximum probability and they constitute 62% of all $n_h=0$ events. Consequently, we deduce that the nuclear structure of the projectile nucleus plays an important role in the fragmentation process.
- 2) The average number of produced charged pions per interacting projectile nucleon is constant at different impact parameters and equals the corresponding value from elementary interaction. This experimental fact supports the hypothesis of considering nucleus-nucleus interaction a super-position of nucleon-nucleon collisions.
- 3) The rapidity distribution of shower tracks from $n_h=0$ events, has its peak in the high rapidity region i.e. the projectile fragmentation region and it is separated by a measurable rapidity gap from the target fragmentation region. These features are related to the limiting fragmentation hypothesis.
- 4) The projected angular distributions of $Z=1$ and $Z=2$ projectile fragments, are Gaussian shaped, narrow, consistent with isotropy of the momentum distribution in the projectile rest frame and depend on the fragment. Invoking the results of measuring the longitudinal momentum distributions from single-particle inclusive experiments, one can deduce that our data of angular distributions demonstrate the validity of limiting fragmentation process in heavy ion collisions at high energy.
- 5) The angular distribution widths are consistent with a quantum mechanical calculations using the sudden approximation and shell-model functions.
- 6) The diffraction dissociation events of $^{12}\text{C} \rightarrow 3\alpha$ are 1.2% of the total inelastic events. The angular distribution of these α -fragments indicates that this reaction goes through an intermediate step of ^8Be .

AKNOWLEDGEMENTS

The author would like to thank the members of Bucharest-Dubna-Kosice-Leningrad-Moscow-Tashkent-Warsaw collaboration for their cooperation during the course of the experiment. He thanks Prof. K.D. Tolostov for his continuous help and for suggesting and discussing the dissociation of carbon projectile nucleus into three alpha-particles. Also, he deeply thanks the authority of Frascati National Laboratories, especially Prof. P. Picchi, for their support.

REFERENCES

1. Frier P., Lofgren E.J., Ney E.P., Oppenheimer F., Brandt H.L. and Peters B.: Phys. Rev. 74, 213 (1948).
2. Waddington C.J.: Prog. Nucl. Phys. 8, 1 (1960).
3. Lohrmann E. and Teucher M.W.: Phys. Rev. 115, 639 (1959).
4. Jain P.L., Lohrmann E. and Teucher M.W.: Phys. Rev. 115, 643 (1959).
5. Rybicki K.: Nuovo Cimento, 28, 1437 (1963).
6. Rybicki K.: Acta Phys. Polonica 36, 69 (1969).
7. Wosiek B.: Acta Phys. Polonica B9, 191 (1978).
8. Vernov S.N., Grigorov N.L. and Chudakov A.E.: Yad. Fiz. 28, 1021 (1978).
9. Gaisser T.K.: J. Franklin Inst. 298, 271 (1974).
10. Grieder P.K.F.: Riv. Nuovo Cimento, 7, 1 (1977).
11. McCusker C.B.A.: Phys. Reports 20C, 59 (1975).
12. El-Naghy A. and Toneev V.D.: Z. Physik A298, 55 (1980).
13. El-Naghy A.: Frascati Report LNF-81/3 (1981), submitted to Nuovo Cimento.
14. Heckman H.H., Greiner D.E., Lindstrom P.J. and Bieser F.S.: Phys. Rev. Letters 28, 926 (1972).
15. Greiner D.E., Lindstrom P.J., Heckman H.H., Cork B. and Bieser F.S.: Phys. Rev. Letters 35, 152 (1975).
16. Lindstrom P.J., Greiner D.E., Heckman H.H., Cork B. and Bieser F.S.: Lawrence Berkeley Laboratory Report LBL-3650 (1975).
17. Heckman H.H., Greiner D.E., Lindstrom P.J. and Shwe H.: Phys. Rev. C17, 1735 (1978).
18. Bucharest - Dubna - Kosice - Leningrad - Moscow - Tashkent - Warsaw Collaboration: Dubna Preprint JINR, E1-10838, (1977).
19. Bradt H.L. and Peters B.: Phys. Rev. 77, 54 (1950).
20. Karol P.J.: Phys. Rev. C11, 1203 (1975).
21. Bucharest - Dubna - Kosice - Leningrad - Moscow - Tashkent - Warsaw Collaboration: Dubna Preprints JINR, P1-6877, (1972); JINR, P1-8313, (1974).
22. Chernov G.M., Gulamov K.G., Gulyamov U.G., Nasyrov S.Z. and Svechnikova L.N.: Nucl. Phys. A280, 478 (1977).
23. Bialas A., Bleszynski M. and Czyz W.: Nucl. Phys. B111, 461 (1976).
24. Lepore J.V. and Riddell R.J.: Lawrence Berkeley Laboratory Report LBL-3086, (1974).